

ANALYTICAL FUNCTION FOR FITTING PEAKS IN ALPHA-PARTICLE SPECTRA FROM Si DETECTORS

G. Bortels and P. Collaers *

Commission of the European Communities, JRC-Geel Establishment,
Central Bureau for Nuclear Measurements, Steenweg naar Retie, B-2440 Geel, Belgium.

ABSTRACT

The performance of an analytical peak-shape function for fitting peaks in alpha-particle spectra has been examined using carefully measured spectra of ^{234}U , ^{241}Am and plutonium. The function used consists of the convolution of a Gaussian and a weighted sum of two left-sided exponentials. Peak fits using this function are performed on spectra from which a tail distribution has previously been subtracted.

INTRODUCTION

Interpolation, often by hand, is currently applied to alpha-particle spectra to correct for peak tailing in the case of well separated peaks or groups of peaks. The method is reliable and allows high accuracy when analysing for ratios of peak areas as described by, e.g., Bortels et al. (1979, 1984) and Glover (1984). The analysis of overlapping peaks, however, not only requires a reliable peak-shape function but also optimal source-preparation procedures and measuring conditions. Although ratios of $^{239}\text{Pu}/^{240}\text{Pu}$ abundances can be measured with far better accuracy by mass spectrometry, there is considerable interest in obtaining reliable results within a few percent by alpha-particle spectrometry.

For the peak-shape function, we have been interested in particular in the analytical function, which was first proposed by L'Hoir (1975) and described by L'Hoir et al. (1976) and Amsel et al. (1976). They used a convolution of a Gaussian and a left-sided exponential to approximate the response of surface-barrier detectors to various mono-energetic light ions, including alpha particles, in the energy range 0.3 to 1.7 MeV. In a later work L'Hoir (1984) examined this model for alpha particles of up to 3.3 MeV. We have tested the peak-shape function for a large number of actinide spectra measured with ion-implanted silicon detectors and adapted it to improve the tail approximation. Usually, special attention is paid to produce spectra of high resolution and minimal deformation. Three examples of analysed spectra are discussed. It should also be mentioned that Wätzig and Westmeier (1978) and Westmeier (1984, 1986) used this function for the term representing the tail portion of peaks in alpha-particle spectra. In gamma-ray spectra from germanium detectors Phillips and Marlow (1976) used it for two such terms.

PEAK-SHAPE FUNCTION

The analytical function for the single alpha peak we are interested in is usually written as a convolution product

$$f(u) = G(u) * E(u) H(-u).$$

Here, u is the energy variable, $G(u)$ represents a normalised Gaussian, $E(u) \cdot H(-u)$ is a left-sided exponential where $H(-u)$ is the left-sided unit-step function defined by $H(-u)=1$ for $-\infty < u \leq 0$, otherwise $H(-u)=0$. The interesting feature of this peak-shape model is that $f(u)$ can be interpreted as a joint-probability-density function. In this context the detection of an alpha particle is thought of as a process in which every event is governed by two mutually independent random variables. One of them is characterized by a symmetric probability-density function and the other one by a purely asymmetric probability-density function. Electronic noise and energy straggling are random processes which belong essentially to the first group whereas incomplete charge collection belongs to the second one.

The explicit expression for the analytical function is obtained as follows. One considers two mutually independent random variables x and y in the energy domain with probability-density functions, respectively,

* Presently at Robert Bosch N.V., B-3300 Tienen, Belgium.

$$p_x(x) = \frac{1}{\sigma\sqrt{2\pi}} \exp\left(-\frac{x^2}{2\sigma^2}\right) \quad -\infty < x < +\infty$$

which represents a normalised Gaussian with standard deviation σ , and

$$p_y(y) = \frac{1}{\tau} \exp\left(-\frac{y}{\tau}\right) H(-y) \quad -\infty < y < +\infty \quad (1)$$

representing a normalized left-sided exponential with parameter τ .

The random variable $u=x+y$ is then characterised by the joint-probability-density function (see e.g. Brandt (1983)).

$$p_u(u) = \int_{-\infty}^0 p_y(y) p_x(u-y) dy. \quad (2)$$

The normalized function of Eq.(2), after integration, takes the form

$$p_u(u) = \frac{1}{2\tau} \exp\left(\frac{u}{\tau} + \frac{\sigma^2}{2\tau^2}\right) \operatorname{erfc}\left[\frac{1}{\sqrt{2}}\left(\frac{u}{\sigma} + \frac{\sigma}{\tau}\right)\right], \quad (3)$$

in which erfc is the complementary error function. Actual peaks in alpha spectra, however, have a peak area A different from unity and their peak position is taken into account by introducing a mean μ into the Gaussian probability-density function. Inserting these parameters into Eq.(3), one obtains the expression for the fitting function

$$f(u) = A p_u(u) = \frac{A}{2\tau} \exp\left(\frac{u-\mu}{\tau} + \frac{\sigma^2}{2\tau^2}\right) \operatorname{erfc}\left[\frac{1}{\sqrt{2}}\left(\frac{u-\mu}{\sigma} + \frac{\sigma}{\tau}\right)\right]. \quad (4)$$

For convenience we will use the following notation, in which the step function is omitted

$$f(u) = A G(u) * E(u). \quad (5)$$

Alpha peak asymmetry is relatively well described by such a model. However, according to our experience, peak tailing in spectra from essentially massless sources measured with ion-implanted detectors is not adequately dealt with by an expression which contains a single exponential asymmetry function. Instead of $E(u)$ in Eq.(5) we therefore adopt a sum of exponentials and a constant. This function is split into a part Ψ_1 , which accounts for the asymmetry in the peak region close to the mode, and another one, Ψ_2 , for the peak tail at lower energies, hence

$$f(u) = A G(u) * [\Psi_1(u) + \Psi_2(u)].$$

This is readily obtained if for $\Psi_1(u)$ one takes the weighted sum of two functions Eq.(1) with parameters τ_1 close to σ and τ_2 roughly three-times larger. The function $\Psi_2(u)$ is a constant with in some cases an extra term for a "long-range" exponential with parameter τ_3 much larger than σ . Consequently

$$\Psi_1(u) = (1-\eta) E_1(u) + \eta E_2(u) \quad (6)$$

$$\Psi_2(u) = C + \varepsilon E_3(u). \quad (7)$$

Here, η and ε are weights and C is a constant.

For a measured spectrum $F(u)$ which is composed of m peaks an approximation by a sum of fitting functions can then be written

$$F(u) = \sum_{i=1}^m f_i(u) + R(u), \quad (8)$$

where $R(u)$ is the distribution of residuals from the fit.

Making use of some properties of convolutions we rewrite Eq.(8), to indicate that first a tail function is subtracted from the measured spectrum, as follows:

$$F(u) - \underbrace{\left(\sum_{i=1}^m A_i G_i(u)\right) * \Psi_2(u)}_{\text{tail function}} = \underbrace{\sum_{i=1}^m A_i G_i(u) * \Psi_1(u)}_{\text{fitting function}} + R(u). \quad (9)$$

Since the tail function is a relatively small correction to the measured spectrum the approximation $\left(\sum_{i=1}^m A_i G_i(u)\right) \approx F(u)$ applies. Furthermore, in this tail subtraction we only consider the constant term in Eq.(7) and put $\epsilon=0$.

Eq.(9) for the spectrum after tail subtraction, $F_C(u)$, can be written as follows

$$F_C(u) = F(u) - \underbrace{F(u) * C}_{\text{tail function}} = \underbrace{\sum_{i=1}^m A_i G_i(u) * \left[(1-\eta) E_1(u) + \eta E_2(u) \right]}_{\text{fitting function}} + R(u), \quad (10)$$

The convolution $F(u)*C$ is calculated numerically and normalized to the height of the flat tail in the spectrum $F(u)$. This procedure does not require any specific information on the spectrum fine structure. A similar tail subtraction prior to spectrum analysis was already used by Wätzig and Westmeier (1978).

The spectrum $F_C(u)$, is subsequently analysed using the fitting function given in Eq.(10) and a nonlinear least-squares procedure to optimize the parameters. According to Eq.(4) the fitting function in Eq.(10) takes the explicit form

$$\begin{aligned} \text{fitting function} = & \sum_{i=1}^m \frac{A_i}{2} \left\{ \left(\frac{1-\eta}{\tau_1} \right) \exp \left(\frac{u-\mu_1}{\tau_1} + \frac{\sigma^2}{2\tau_1^2} \right) \operatorname{erfc} \left[\frac{1}{\sqrt{2}} \left(\frac{u-\mu_1}{\sigma} + \frac{\sigma}{\tau_1} \right) \right] \right. \\ & \left. + \frac{\eta}{\tau_2} \exp \left(\frac{u-\mu_1}{\tau_2} + \frac{\sigma^2}{2\tau_2^2} \right) \operatorname{erfc} \left[\frac{1}{\sqrt{2}} \left(\frac{u-\mu_1}{\sigma} + \frac{\sigma}{\tau_2} \right) \right] \right\}. \quad (11) \end{aligned}$$

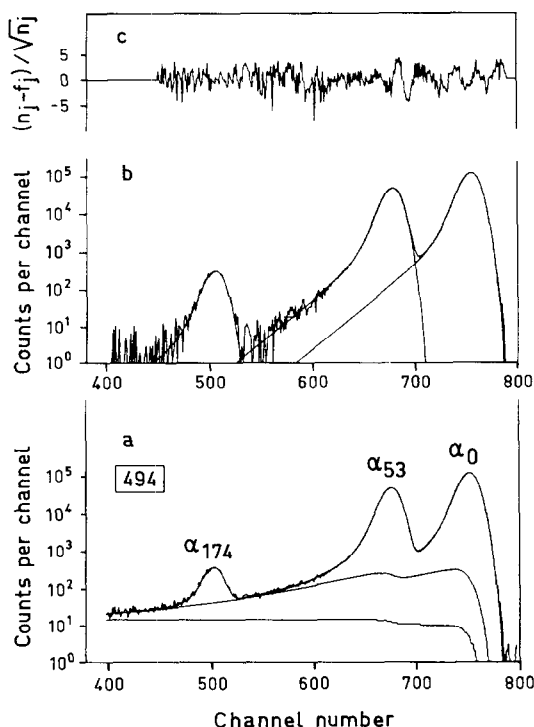


Fig.1. a) Alpha-particle spectrum of ²³⁴U showing two different tail functions (see text) and the fitted spectrum; b) analysed peaks in the spectrum after tail subtraction; c) weighted residuals from the peak fits.

This is a function of 4 shape parameters $\sigma, \tau_1, \tau_2, \eta$, which are the same for all peaks in the fit, in addition to two parameters A_i, μ_i , specific for each peak.

If $F_C(u)$ shows a "long-range" exponential to be present, one may proceed to a further tail subtraction involving the second term $\epsilon E_2(u)$ of Eq.(7). The two parameters of $\epsilon E_2(u)$, which are required for this tail subtraction, can be obtained from a fit in which $\eta E_2(u)$ is optimized for the tail region of $F_C(u)$ where the steeper exponentials $E_1(u)$ and $E_2(u)$ have negligible contributions. In fact, for this latter tail correction we found that it is not strictly necessary to make use of the full fine structure present in the spectrum $F_C(u)$. For this purpose a group of peaks in the spectrum can be replaced by a single peak having about the same number of counts as that in the group, a peak position close to the centroid of the group and approximate parameters σ and τ_1 obtained in the first fit.

In a number of cases the second tail subtraction may require some trial and error to improve the fit. In practice, the optimized parameters τ_2 and η depend on the region selected for the fit. The long-range tail function has therefore to be judged by visual inspection. The decision whether or not a "long-range" tail subtraction will be made is therefore often a matter of how much effort one is prepared to spend on the analysis of a given spectrum. The long-range exponential $\epsilon E_2(u)$ could easily be built into the fitting function if wanted.

ANALYSIS OF SPECTRA

To test the peak-shape function Eq.(11), we have analysed spectra from ^{234}U , ^{241}Am and the NBS plutonium standard reference material SRM 947.

The ^{234}U spectrum had been collected in the course of an earlier project when the alpha-particle emission probabilities of this nuclide were measured with high accuracy (Vaninbroukx et al. (1984)). It has been chosen for its large number of counts and well controlled measurement conditions. The source had an activity of 1536 Bq contained in a spot of 8 mm in diameter. It had been prepared on a stainless-steel disc by sublimation of highly pure material in vacuum. A resolution of 13.2 keV, full width at half maximum (FWHM), was obtained in the measurement using a detector of 20 mm² active area. The source-to-detector geometry was 0.4% of 4 π sr. A small permanent magnet was used to deflect conversion electrons (CE) away from the detector. In this way peak deformation resulting from α -CE summing was reduced (Bortels (1984)). The spectrum is the sum of 41 measurement cycles of 2h each. Prior to adding these spectra together the position of the major peak in each spectrum was fitted and, if required, matched by shifting spectra over an integer number of channels. In this way amplifier-gain drift was partly corrected for, which resulted in an improved peak resolution. With an energy scale of 0.69 keV per channel a peak broadening of this magnitude could, however, not be excluded.

Fig.1a shows the measured spectrum and two tail functions. The lower curve corresponds to the tail function for which $\epsilon=0$, whereas in the other one an optimized value for ϵ has been used. Peak fits have been made on the spectrum obtained after subtraction of the latter tail function (Fig.1b). The fitted spectrum is also shown as a full line in Fig.1a. The two major peaks a_0 and a_{53} were fitted in the region from channel 610 to 788. The reduced chi-square value is generally used to quote the quality-of-fit. It is expressed as

$$\chi_R^2 = \frac{1}{N} \sum_{j=r}^k \frac{(n_j - f_j)^2}{n_j}, \quad (12)$$

where n_j is the number of counts in channel j and f_j is the value of the function at that channel. For a fit region from channel r to k the number of degrees of freedom is given by $N=k-r+1-N_p$ where N_p is the number of parameters in the fit. The χ_R^2 obtained for the fit of the two major peaks is 3.0. The parameters A and μ of the minor peak a_{174} were subsequently fitted in the region from channel 450 to 529 whilst fixing the shape parameters σ , τ_1 , τ_2 , η , at the values obtained in the fit of a_0 and a_{53} . All fits were made applying weights $W_j=1/n_j$ to the spectral data. It should be noted that all peak positions are a few channels lower than the corresponding μ_i values as a result of the convolution.

Since there are no other peaks in the spectrum, the relative peak areas obtained from the fits are an approximation of the alpha-emission probabilities of this nuclide. The results are shown in Table 1. Uncertainties in units of the last decimal figure are put in brackets. For the results from the fits the quoted uncertainties result from the variance-covariance matrix of the optimized parameters for a 75 percent confidence interval. The same confidence interval was used in the analysis of the other spectra. For the P_a values the uncertainties were taken from the IAEA (1986) evaluation and correspond to one standard deviation of the mean. The results are in perfect agreement with each other as well as with our earlier results (Vaninbroukx et al. (1984)). Fig.1c shows the weighted residuals from the fits of the peaks. The apparent structure at energies above that of the a_{53} peak is not yet identified.

Table 1. Comparison of relative peak areas $A_i/\Sigma A_i$ from a fitted ^{234}U alpha-particle spectrum and emission probabilities P_a from the IAEA (1986) evaluation.

Peak	Energy $E_a(\text{keV})$	$A_i/\Sigma A_i$	χ_R^2	P_a
a_{174}	4603.8	0.0020(1)	3.0	0.00199(2)
a_{53}	4722.6	0.2842(9)		0.2842(2)
a_0	4774.9	0.7138(16)		0.7137(2)

Table 2. Comparison of relative peak areas $A_i/\Sigma A_i$ from a fitted ^{241}Am alpha-particle spectrum and emission probabilities P_a from the IAEA (1986) evaluation.

Peak	Energy $E_a(\text{keV})$	$A_i/\Sigma A_i$	χ_R^2	P_a
$a_{158.5}$	5388.	0.016(1)	4.0	0.014(2)
a_{103}	5442.9	0.130(3)		0.128(2)
$a_{59.5}$	5485.6	0.847(9)		0.852(8)
a_{33}	5512.	0.0022(3)	1.3	0.0020(5)
a_0	5544.	0.0034(4)		0.0034(5)

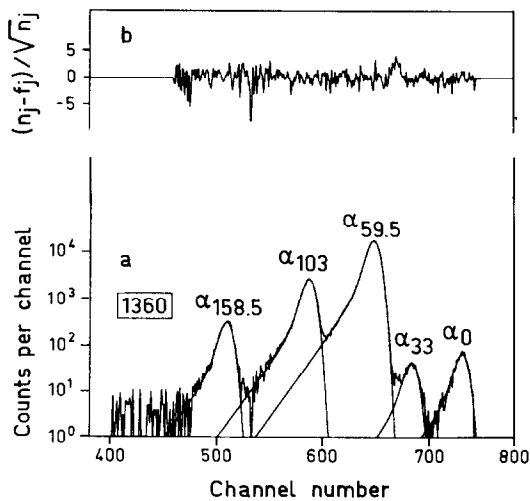


Fig. 2. a) Alpha-particle spectrum of ^{241}Am after a tail subtraction and analysed peaks; b) weighted residuals from the fits.

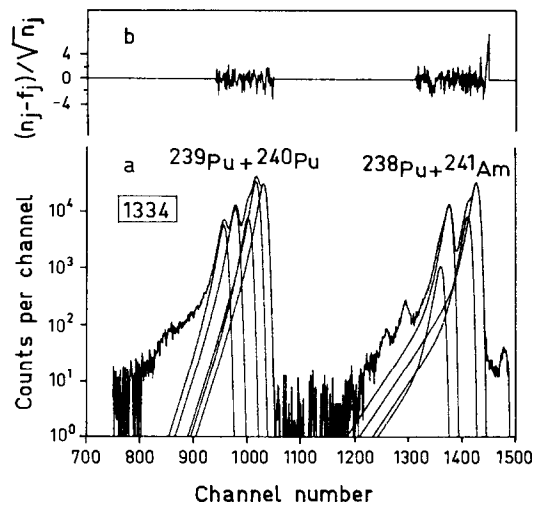


Fig. 3. a) Analysis of the plutonium spectrum from a sample of NBS SRM 947. The ^{241}Am has grown into the source over a period of 2.643 years; b) weighted residuals from the fits.

The ^{241}Am spectrum used in the present work was chosen for its very high peak resolution of 9.0 keV FWHM. A vacuum-sublimed source on a glass disc was used in the measurement. The source activity was 4600 Bq and the spot diameter about 10 mm. Here, a detector of 50 mm² area and 300 μm depletion depth from Canberra Semiconductor N.V. (B-2430, Olen, Belgium) has been used. The measurement geometry was 0.35 % of 4π sr and the energy scale 0.70 keV per channel. Again, a magnetic field was used to deflect conversion electrons. Furthermore, the detector and preamplifier were operated at a constant temperature of 21°C and a vacuum of 1.3×10^{-2} Pa was maintained during the measurement. About 3×10^5 counts were collected in the spectrum. The spectrum shown in Fig.2a was obtained after subtracting a tail function (Eqs.(9) and (7)), for which $\varepsilon \neq 0$, from the measured spectrum. The peak-shape parameters $\sigma, \tau_1, \tau_2, \eta$ together with the peak areas A_i and positions μ_i of the two major peaks have been optimized in the region from channel 534 to 666. Here, a value $\chi_R^2 = 1.9$ was obtained. For the remaining peaks the peak-shape parameters were kept fixed and only peak areas and positions were optimized. The peaks a_0 and a_{33} were fitted in the region from channel 670 to 742 and $a_{158.5}$ in the region 460 to 529. Table 2 shows the relative peak areas obtained in the fit and, for comparison, also the alpha-emission probabilities for ^{241}Am according to the IAEA (1986) evaluation. Uncertainties have the same meaning as in Table 1. Again, there is perfect agreement between the data. Fig.2b shows the weighted residuals from these fits. A small residual peak can be seen.

The spectrum of the plutonium NBS SRM 947 used in this work has been obtained in a routine measurement. This material was chosen for its well documented characterization values (NBS (1982)) and alpha activity ratio $^{238}\text{Pu}/^{239+240}\text{Pu}$ (Bortels and Verbruggen (1984)). An old source, prepared on stainless steel by drop deposition and using tetraethyleneglycol as a seeding agent, was used in the measurement. At the time of source preparation, March 5th 1984, ^{241}Am had been removed by anion exchange. The source was measured 2.643 years later and the ^{241}Am grown into it was calculated from the ^{241}Pu content as given in the NBS certificate. The source activity was about 4890 Bq. A detector of 25-mm² active area and 300- μm depletion depth was put in a geometric arrangement of about 0.7 % of 4π sr. The energy scale was 0.84 keV per channel and the resolution 11.9 keV FWHM. About 2.5×10^6 counts were collected in the spectrum.

The spectrum shown in Fig.3a was obtained after subtraction of a tail function, in which $\varepsilon \neq 0$. The peak-shape parameters $\sigma, \tau_1, \tau_2, \eta$ were optimized separately for the two groups $^{239+240}\text{Pu}$ and $^{238}\text{Pu} + ^{241}\text{Am}$. In the $^{239+240}\text{Pu}$ group, five peaks have been fitted in the region from channel 940 to 1048. These peaks account for about 99.9 % of the alpha-particle emission rate for these nuclides. Results have been corrected for the 0.1 % unaccounted for. For the $^{238}\text{Pu} + ^{241}\text{Am}$ group the fit was limited to the four major peaks in the region from channel 1310 to 1444. These peaks account for about 99.9 % of the ^{238}Pu and 98 % of the ^{241}Am emission rate, for the remainder of which corrections have been made. For the $^{239+240}\text{Pu}$ group the first channel of the fitting region has been intentionally chosen closer to the peaks than in the case of the $^{238}\text{Pu} + ^{241}\text{Am}$ group to show the influence on the tail of the fitted peaks. By applying similar fitting regions for both groups the $^{238}\text{Pu}/^{239}\text{Pu}$ result lowers 0.6 %. Fig.3b shows the weighted residuals from the fits.

Table 3. Relative peak areas $A_i/\Sigma A_i$ and deduced activity and atom ratios from a fitted plutonium alpha-particle spectrum of the NBS SRM 947. Results are compared with emission probabilities P_a and data calculated from the NBS certificate of plutonium isotopic analysis.

Nuclide	Energy E_a (keV) ¹⁾	$A_i/\Sigma A_i$	χ^2_R	P_a ¹⁾	Activity ratio	Atom ratio
^{241}Am	5442.9	0.115(7)	2.4	0.128(2)	$^{241}\text{Am}/^{238}\text{Pu} =$	$^{238}\text{Pu}/^{239}\text{Pu} =$
	5485.6	0.866(20)		0.852(8)	0.210(6)	$3.59(6) \cdot 10^{-3}$
					0.228(2) ²⁾	$3.48(4) \cdot 10^{-3}$ ²⁾
^{238}Pu	5456.5	0.286(4)	1.2	0.2884(6)	$^{238}\text{Pu}/^{239}+^{240}\text{Pu} =$	$^{240}\text{Pu}/^{239}\text{Pu} =$
	5499.21	0.713(6)		0.7104(6)		
^{239}Pu	5105.5	0.121(2)	1.2	0.118(2)	$^{238}\text{Pu}/^{239}+^{240}\text{Pu} =$	$^{240}\text{Pu}/^{239}\text{Pu} =$
	5143.8	0.167(5)		0.150(2)		
	5156.7	0.712(7)		0.731(7)		
^{240}Pu	5123.68	0.272(4)	1.2	0.270(5)	0.519(9)	0.245(5)
	5168.17	0.727(9)		0.729(5)	0.509(1) ³⁾	0.2410(1) ²⁾

1) Data from the IAEA (1986) evaluation.

2) Calculated from the NBS-certificate values, using half lives from the IAEA (1986) evaluation.

3) Value from Bortels and Verbruggen (1984) corrected for decay as of October, 1986.

Results from the fits are reported in Table 3, where alpha-emission probabilities are given for comparison. From these data alpha-particle activities relative to that of either ^{238}Pu or $^{239}+^{240}\text{Pu}$ were obtained. For peaks with a peak ratio of about 1/4 and an energy separation of about one FWHM it is found that the peak ratio obtained in the fit differs from the target value by about 15 %. This figure provides an estimate for the possible deviation of the area of the smaller of the two peaks from the "true" value in cases where the number of counts in the peak is relatively large. Examples for this case are the two large peaks of ^{239}Pu and the major peaks of ^{241}Am and ^{238}Pu . Furthermore, the activity ratios show that the overestimation of $^{238}\text{Pu}/^{239}+^{240}\text{Pu}$ is due to the underestimated $^{241}\text{Am}/^{238}\text{Pu}$.

Atom ratios of plutonium isotopes relative to that of ^{239}Pu were also deduced. The sum of the two large peaks of ^{239}Pu is usually obtained with good accuracy and enters into the $^{240}\text{Pu}/^{239}\text{Pu}$ ratio. The deviation (less than 2 %) of the $^{240}\text{Pu}/^{239}\text{Pu}$ result from the target value is rather typical in case of analysing for the ratio of equally large peaks having an energy separation of about one FWHM.

Variances for ratios were taken as the sum of variances of the elements. Uncertainties given in the NBS certificate have been arbitrarily divided by a factor 2 in order to compare roughly at the 75 % confidence level. Half-life values from the IAEA (1986) evaluation have been used throughout.

CONCLUSION.

An analytical function to fit peaks in alpha-particle spectra has been deduced from the convolution model proposed by L'Hoir (1975). Exponential terms and a constant have been added to the original model to improve the fit. The analysis of ^{234}U , ^{241}Am and plutonium spectra shows that the proposed peak-shape function performs reliably and allows peak ratios to be measured accurately. Different ion-implanted detectors without additional diaphragm and two different source-preparation techniques were used.

For partly separated peaks in spectra with small tailing, relative peak areas obtained in the fits were found to fully agree with results from accurate measurements and evaluated data. For plutonium spectra with relative activities of the nuclides close to 1 the agreement between nuclide-activity ratios obtained in the fit and target values is found to be 1 to 3 percent.

For other isotopic compositions and for other nuclides accuracies should be investigated for a number of typical spectra. It is therefore useful to produce reference alpha spectra using very stable electronics and well controlled measuring conditions. The present peak-shape function should enable accurate measurement of the alpha-particle-emission probabilities in complex spectra such as e.g. ^{237}Np .

For applications where a high accuracy is not a major requirement some of the parameters in both the fit function and the tail function could be omitted.

The best reduced chi-square values obtained in our fits seem to approach those reported by Campbell et al. (1985), Helmer and Lee (1980) and Watanabe et al. (1986) for peak fits in gamma-ray spectra from Ge semiconductor detectors and X-ray spectra from Si(Li) detectors.

REFERENCES

- Amsel G., C. Cohen and A. L'Hoir (1976), in Proc. Int. Conf. on Ion Beam Surface Layer Analysis, Karlsruhe, Germany, Sept. 15-19, 1975, Vol.2, 953 (Eds. O. Meyer, G. Linker and F. Käppeler, Plenum, New-York).
- Bortels G., P. De Bièvre, L. Barnes and K.M. Glover (1979) in Proc. First Ann. Symp. on Safeguards and Nuclear Material Management. European Safeguards Research and Development Association (ESARDA), Brussels, Belgium, April 25-27, 1979, 380 (Ed. L. Stanchi, Commission of the European Communities, JRC-Ispira, Italy).
- Bortels G., D. Reher and R. Vaninbroux (1984). Int. J. Appl. Radiat. Isot. **35**, 305.
- Bortels G., (1984) in Ann. Progress Report on Nuclear Data 1983, 81. NEANDC (E) 252 "U", Vol. III Euratom, INDC(EUR)018/G, Central Bureau for Nuclear Measurements, Geel, Belgium.
- Bortels G. and A. Verbruggen (1984) in Proc. Sixth Ann. Symp. on Safeguards and Nuclear Material Management. European Safeguards Association (ESARDA), Venice, Italy, May 14-18, 1984, 431 (Ed. L. Stanchi, Commission of the European Communities, JRC-Ispira, Italy).
- Brandt S. (1983), Statistical and Computational Methods in Data Analysis, (2nd ed., North Holland), p. 82.
- Campbell J.L., B.M. Millman, J.A. Maxwell, A. Perujo and W.J. Teesdale (1985). Nucl. Instrum. Methods Phys. Res. **B9**, 71.
- Glover, K.M. (1984). Int. J. Appl. Radiat. Isot. **35**, 239.
- Helmer R.G. and M.A. Lee (1980). Nucl. Instrum. Methods **178**, 499.
- IAEA (1986). Decay Data of the Transactinium Nuclides, International Atomic Energy Agency, Technical Report Series No.261.
- L'Hoir (1975). Thèse 3ème cycle, Université Paris 7, unpublished.
- L'Hoir A., C. Cohen and G. Amsel (1976) in Proc. Int. Conf. on Ion Beam Surface Layer Analysis, Karlsruhe, Germany, Sept. 15-19, 1975, Vol.2, 965 (Eds. O. Meyer, G. Linker and F. Käppeler, Plenum, New-York).
- L'Hoir A. (1984). Nucl. Instrum. Methods Phys. Res. **223**, 336.
- NBS (1982). National Bureau of Standards, Certificate of Analysis, Standard Reference Material 947, Washington D.C. 20234.
- Phillips G.W. and K.W. Marlow (1976). Nucl. Instrum. Methods **137**, 525.
- Vaninbroux R., G. Bortels and B. Denecke (1984). Int. J. Appl. Radiat. Isot. **35**, 1081.
- Watanabe Y., T. Kubozoe and T. Mukoyama (1986). Nucl. Instrum. Methods Phys. Res. **B17**, 81.
- Wätzig W. and Westmeier W. (1978). Nucl. Instrum. Methods **153**, 517.
- Westmeier, W. (1984). Int. J. Appl. Radiat. Isot. **35**, 263.
- Westmeier, W. (1986). Nucl. Instrum. Methods Phys. Res. **A242**, 437.